Decaying and kicked turbulence in a shell model

Jan-Otto Hooghoudt, Detlef Lohse*, and Federico Toschi

Department of Applied Physics and J. M. Burgers Centre for Fluid Dynamics, University of Twente, P. O. Box 217, 7500 AE Enschede, The Netherlands

Decaying and periodically kicked turbulence are analyzed within the GOY shell model, to allow for sufficiently large scaling regimes. Energy is transfered towards the small scales in intermittent *bursts*. Nevertheless, mean field arguments are sufficient to account for the ensemble averaged energy decay $E(t) \sim t^{-2}$ or the parameter dependences for the ensemble averaged total energy in the kicked case. Within numerical precision, the inertial subrange intermittency remains the same, whether the system is forced or decaying.

I. INTRODUCTION

Three dimensional turbulent flows are characterized by a highly chaotic and intermittent transfer of energy from the outer length scale down to the dissipative, inner length scale. In this paper we will focus on two different kinds of turbulent flows: Decaying turbulence and periodically kicked turbulence. Both types of flow have already been analysed within a mean field theory [1,2], but here we would like to focus also on intermittency effects which cannot be described in the mean field approach [3].

To be more specific: With *decaying turbulence* we mean a homogeneous and isotropic turbulent flow for which forcing is ceased from some time t_0 on. Therefore, eventually all the energy will be damped because of dissipative effects, but the statistical properties of the decaying turbulent field are a priori not clear. With periodically *kicked turbulence* we mean a turbulent field forced with short and very strong periodic pulses.

The motivation of the paper is to study the effect of non-trivial forcing on the properties of the turbulence. Most numerical or theoretical studies assume a Gaussian random noise forcing, acting on the largest scales only. But for most practical flows the forcing protocol is obviously more complex and often periodic, be it pulsed flow through a pipeline or the earth's atmosphere driven by the periodical heating through the sun. Another example of periodically kicked turbulence is the numerical realization of homogeneous shear flow [4] where periodical remeshing is necessary. In between the kicks the turbulence is supposed to be freely decaying. Therefore an understanding of decaying turbulence is required. Beyond this, decaying turbulence is of course one of the classical examples of turbulent flow and an extended literature exists, see e.g. [5–9].

The aim of the paper is to explore the statistical properties of turbulence both in the decaying and kicked case. Therefore, we must have excellent statistics. This turns out to be prohibative in a direct numerical simulation (DNS) of the Navier-Stokes equation and that is why we revert to study the problem in the context of the GOY shell model of turbulence [10] in which a scaling regime of many decades can be achieved. To our knowledge the present study is the first on the classical problem of decaying turbulence with the help of a shell model.

Shell models are defined by a set of hierachically coupled ODEs for the velocity modes

which try to reproduce the physics of the energy flux of Navier-Stokes equation. The dynamical equations for the GOY models read [10–13]

$$\left(\frac{d}{dt} + \nu k_n^2\right) u_n = ik_n \left(a_n u_{n+2} u_{n+1} + b_n u_{n+1} u_{n-1} + c_n u_{n-1} u_{n-2}\right)^* + g\delta_{n,0} \tag{1}$$

were $n = 0, \ldots, N - 1$, $k_n = 2^n k_0$, $a_n = 1$, $b_n = -\delta/2$ and $c_n = -(1 - \delta)/4$ and the boundary conditions are $a_{N-1} = a_N = b_N = b_1 = c_1 = c_2 = 0$ in order for the GOY model to conserve the energy in the unforced and inviscid case ($g = \nu = 0$). Traditionally, the free parameter δ is chosen to be $\delta = 1/2$. The values of the other parameter used were $N = 22$, $g = (1 + i) \cdot 10^{-2}$, and $\nu = 10^{-6}$.

II. DECAYING TURBULENCE: GLOBAL PROPERTIES

The stationary (i.e. forced) simulations of eq. (1) were performed using fourth order Runge-Kutta with viscosity explicitly integrated. For the decay run we used the same algorithm but increased the time step keeping it $1/10$ of the dissipative time scale. During the decay process indeed the dynamics becomes slower and slower and investigation of long time properties is only possible using a scheme with an adaptive time step.

We performed a very long stationary simulation of equation (1) from which we collected an ensemble of starting configurations (~ 2500 independent runs) for studying the free decay of GOY turbulence. The starting configurations of the ensemble were collected after some eddy turnover time in order to be statistically independent. We let each of the starting configurations decay according to equation (1) (i.e. with $g = 0$ and all other parameters unchanged).

During the decay stage we measure the total energy $E(t) = \sum_{n=0}^{N-1} |u_n(t)|^2$ as a function of the decay time t (the time elapsed from when we switched off the forcing). In figure 1 the decay of the total energy on a *single* run is shown, i.e., no ensemble average is performed here. The total energy decays in burst, i.e., it is constant for some time and than very suddenly drops. As this behavior occurs on all scales, the step-like structure looks self similar. The averaged (over the whole decay) decay exponent is close to -2. For very large times it decays exponentially. The derivative of the energy decay is shown in figure 2 in order to better highlight the bursty structure. Also from figure 2 one can immediately realize that the typical time scales during the decay becomes larger and larger. The bursty structure of the energy decay in the GOY model has been analyzed in detail by Okkels and Jensen [14, 15] and it reflects the intermittent behavior of the energy flux downscale.

We now *ensemble average* $E(t)$ by collecting various starting configurations as described above and letting them decay. In figure 3 we show the time decay of the ensemble-averaged total energy. The step like behavior of a single realization of $E(t)$ is now completely smeared out and the decay law $\langle E(t) \rangle \sim t^{-2}$ is revealed. For large times the averaged decay is of course again exponential.

We now set up a simple model which is able to describe the *average* energy behavior during the decay process. The model closely follows the mean-field model of reference [1]. The major assumption we make is to suppose that all the energy is contained in the smallest shells corresponding to the largest scales. For simplicity we assume that it is only in the

zeroth shell of eq. (1), $E \simeq \left\langle |u_0|^2 \right\rangle$. During the first part of the decay energy will disappear from the zeroth shell by being transferred to smaller scales $\frac{d}{dt}\left\langle |u_0|^2 \right\rangle \sim -\left\langle |u_0|^3 \right\rangle$ and hence $\frac{d}{dt}\left\langle E(t) \right\rangle \sim -\left\langle E(t) \right\rangle^{3/2}$ with the solution

$$\langle E(t) \rangle = \left[E(t_0)^{-1/2} + \frac{1}{2}(t - t_0) \right]^{-2}. \tag{2}$$

Notice that asymptotically this means that, for $t \gg t_0$, we expect the energy to decay quadratically in time, $\langle E(t) \rangle \sim t^{-2}$, just as seen in figure 3. The reason that the mean field argument works for the averaged decay is that the required time for the transport of pulses downscale is determined by the large scale dynamics, see e.g. figure 1b of Schörghofer [16].

As energy is removed from the system the effective Reynolds number will decrease further and further. In particular there will come a time, t_1, for which even on the zeroth shell the dissipative term will dominate with respect to the non linear term in equation (1). From that moment on, the equation for the energy decay will be $\frac{1}{2}\left\langle |\dot{u}_0|^2 \right\rangle \simeq -\nu k_0^2 \left\langle |u_0|^2 \right\rangle$ and hence $\frac{d}{dt}\left\langle E(t) \right\rangle \sim -\nu k_0^2 \left\langle E(t) \right\rangle$ whose solution is an exponential damping,

$$\langle E(t) \rangle = E(t_1) \cdot \exp\left[-2\nu k_0^2 (t - t_1) \right]. \tag{3}$$

As seen from figure 3, equations (2) and (3) correctly describe the respective short and long term behavior of the energy decay.

III. INTERMITTENCY IN DECAYING TURBULENCE

The time behavior of an individual decay process is complicated because of the bursty structure of the decay, see figure 2. The presence of bursts is an essential feature of intermittency. During the decay process both the intensities of the bursts decrease and their duration increase orders of magnitudes.

The question now is if or not the statistical properties of the turbulent fluctuations remain the same during the decay process. To answer this question we study the k-scaling of higher order moments. Rather than calculating the scaling of moments of the velocity u_n itself, which within the GOY model shows unphysical period 2 and period 3 oscillations [13], we focus on the scaling of energy flux moments [13] $\Sigma_{n,p}$,

$$\Sigma_{n,p}(t) = \left\langle \left| \mathcal{I}\left(u_n u_{n+1} u_{n+2} + \frac{1}{4}u_{n-1}u_n u_{n+1} \right) \right|^p \right\rangle. \tag{4}$$

Here $\mathcal{I}$ denotes the imaginary part. The $\Sigma_{n,p}$ are free of the period 2 and period 3 artifacts in the spectrum and show very clean scaling properties [13]. With the angular brackets $\langle \ldots \rangle$ we again denote ensemble average conditioned to a given decay time t. However, to obtain better statistics, here we had in addition to average over a short period of time. We chose a tenth of a decade and the given times refer to the *end* of that small time interval.

The numerical results are shown in figure 4 where we have plotted various moments of the fluxes as a function of decay time. One evident feature is the decrease of the Reynolds number as the decay goes on. This results from the strong increase of the dissipative scale

and consequently the shortening of the inertial range. In the remaining inertial subrange (ISR) the slope looks very similar, but whether it really is the same cannot yet be judged from this type of plot.

Therefore, in order to explore whether the scaling in the forced and in the unforced cases are really the same, we calculate the ratio between powers of the fluxes computed at different decay times, see figure 5. Though in the forced case the forcing is limited to the zeroth shell, slight deviations spread over the first three shells or so. However, in the ISR the scaling properties and thus the intermittency really seem to be the same, within statistical errors. Note that getting this conclusion from DNS would be very hard, due to the small extension of the inertial subrange.

This result on the lack of dependence of intermittency on the forcing resembles analogous conclusions from analysing the effect of the viscous subrange on the ISR scaling: For both the GOY model and also for DNS She and coworkers [17, 18] found the same degree of ISR intermittency, independently of whether normal or hyperviscosity was employed. Only slightly beyond the onset of turbulence there may be a small dependence on the type of viscosity within the GOY model [19].

IV. KICKED TURBULENCE

Kicked turbulence has been analysed within the framework of a mean-field theory [2]. In the kicked case the GOY model is forced with a delta-like (in time) forcing $g\delta_{n,0}$ with frequency f. With delta-like forcing we mean that the forcing $g\delta_{n,0}$ is periodically turned on for a small time $\Delta t_{kick} \ll f^{-1}$. The presence of the forcing will sustain the energy flux. The turbulence level achieved in kicked turbulence depends on both the forcing strength $A = g\Delta t_{kick}$ and the forcing frequency f. We employ the GOY model dynamics to explore this dependency beyond the simple mean field approach of reference [2].

The qualitative behavior of the energy, as a function of kicking frequency can be seen from figures 6. In figure 6a we can see the energy behavior in the laminar regime. After each kick the system jumps at (almost) constant upper levels. From this value it then decays for a long period before another kick is applied.

In figure 6b we are in the transition regime towards turbulence. The time between two kicks has been decreased as compared to Fig. 6a and hence the system does not have sufficient time to fully relax. The kicks still heavily influence the macroscopic behavior.

In figure 6c the kicking frequency has been further increased and we are close to the turbulent regime. We see regions where the energy starts to pile up for a while, after which it relaxes very fast through bursts of energy. The macroscopic energy behavior is described by a competition between the kicking (with timescale $1/f$) and the energy decay between the kicks (with the time scale of the large eddy turnover time).

In figure 6d we are in the fully turbulent regime. Here the individual kicks are no longer important for the macroscopic energy behavior and they acts as a sort of average constant forcing. Energy can build up over many kicking timescales before it is released through an energy burst, whenever the phase relation is appropriate [14]. This behavior is the analog to the bursty structure of figures 1 and 2 in the decaying case: Energy can only be transported downscale if the phase relations happen to be appropriate [14]. If not, an energy plateau forms in the decaying case or the energy piles up in the kicked case.

To get the dependence of the total energy just before the kick (E_l) and just after the kick (E_u) as a function of the kicking frequency and the kicking strength we again performed ensemble averages of many realizations. In figure 7 we show E_l and E_u as a function of f for three different forcing strengths A. Just as in the mean field case [2] three regimes can be seen: (i) A laminar regime in which the upper energy level is constant and corresponds to the total energy input during the kick and where the time between the kicks is sufficiently large so that the energy completely decays; (ii) a transitional regime; and (iii) a turbulent regime where the average upper and lower energy level are equal as the forcing is experienced as a continuous forcing. The energy levels roughly scale with f^1. In the last regime the features are different from those of the third regime in the mean field theory [2] where the average energy of the lower level is always less than that of the upper level. The reason is that in the dynamical model energy can build up over many forcing periods due to phase blocking. Therefore, it is experienced as a continuous forcing.

Nevertheless, at least the scaling can be obtained by a similar argument as employed in the mean field theory [2]: If the energy of the GOY can be (roughly) approximated by the energy contained in the largest shell, $E_l \sim \langle|u_0|^2\rangle$, then directly after the kick it will be $E_u \sim \langle|u_0 + g\Delta t_{kick}|^2\rangle = \langle|u_0 + A|^2\rangle = E_l + 2A\sqrt{E_l} + A^2$. Between two kicks the system is freely decaying. Therefore we can apply in between two kicks the mean field result of refs. [1, 2] to connect E_u and E_l. If the decay starts from an energy value E_u, after a time $1/f$, when the next kick is applied, the energy will be decayed to E_l. The two energy levels are connected through the equation [1, 2]

$$\frac{1}{f\tau} = 3\left[F(Re(E_l)) - F(Re(E_u))\right]. \tag{5}$$

Here the function $F(Re)$ is defined as [1]

$$F(Re) = \frac{1}{2Re^2}\left\{-\gamma + \sqrt{\gamma^2 + Re^2}\right\} + \frac{1}{2\gamma}\left\{\frac{\gamma + \sqrt{\gamma^2 + Re^2}}{Re}\right\} \tag{6}$$

with $\gamma = 9$. The Reynolds number and the energy in the GOY are connected by $Re(E(t)) = \sqrt{\frac{2}{3}}\frac{L\sqrt{E(t)}}{\nu}$. Here, L is the integral scale and $\tau = L^2/\nu$ a viscous time scale.

Solving equation (5) we can find the value of the upper, E_u, and lower, E_l, energy levels as a function of the forcing strength A and frequency f. In figure 8 this dependence is plotted, revealing the basic features as in the numerical figure 7. For large $Re \gg \gamma$, we have $F(Re) = 1/Re$ and one finds $E_u \sim E_l \sim f$, just as in the numerical case.

V. CONCLUSIONS

We summarize our main findings:

The GOY model is employed to study both decaying and periodically kicked turbulence. Energy is transfered towards the small scales in intermittent *bursts*, leading to stepwise behavior in the decaying case or energy pileups and subsequent bursts in the kicked case. In spite of this intermittent behavior, mean field arguments as developed in refs.[1, 2] are sufficient to account for the ensemble averaged energy decay $\langle E(t)\rangle \sim t^{-2}$ or the parameter dependence $E_u \sim E_l \sim f$ for the ensemble averaged total energy in the kicked case. The

reason that mean field arguments work here is that the decay and the kicking is determined by the large scale dynamics.

For what concerns the statistical properties of decaying turbulence, our finding supports the idea that decaying turbulence has the same intermittency as stationary turbulence. In particular this finding allows to conclude that at least in the GOY model ISR intermittency is independent on the forcing mechanism of turbulence. The only relevant dynamics during the decay process seems to be a shortening of the inertial range (decrease of Reynolds number) but leaving the same intermittency properties.

ACKNOWLEDGMENTS

* Corresponding author

[1] D. Lohse, Phys. Rev. Lett. **73**, 3223 (1994).
[2] D. Lohse, Phys. Rev. E **62**, 4946 (2000).
[3] H. Effinger and S. Grossmann, Z. Phys. B **66**, 289 (1987).
[4] A. Pumir, Phys. Fluids **8**, 3112 (1996).
[5] J. O. Hinze, *Turbulence* (McGraw-Hill, New York, 1975).
[6] A. S. Monin and A. M. Yaglom, *Statistical Fluid Mechanics* (The MIT Press, Cambridge, Massachusetts, 1975).
[7] M. Smith, R. J. Donelly, N. Goldenfeld, and W. F. Vinen, Phys. Rev. Lett. **71**, 2583 (1993).
[8] G. L. Eyink and D. J. Thompson, Phys. Fluids **12**, 477 (2000).
[9] S. R. Stalp, L. Skrbek, and R. J. Donnelly, Phys. Rev. Lett. **82**, 4381 (1999).
[10] T. Bohr, M. H. Jensen, G. Paladin, and A. Vulpiani, *Dynamical Systems Approach to Turbulence* (Cambridge University Press, Cambridge, 1998).
[11] M. H. Jensen, G. Paladin, and A. Vulpiani, Phys. Rev. A **43**, 798 (1991).
[12] D. Pisarenko *et al.*, Phys. Fluids A **5**, 2533 (1993).
[13] L. Kadanoff, D. Lohse, J. Wang, and R. Benzi, Phys. Fluids **7**, 617 (1995).
[14] F. Okkels and M. H. Jensen, Phys. Rev. E **57**, 6643 (1997).
[15] F. Okkels, nlin.CD/0008032 (unpublished).
[16] N. Schörghofer, Eur. Phys. J. B direct **1**, 1 (1998).
[17] E. Leveque and Z. S. She, Phys. Rev. Lett. **75**, 2690 (1995).
[18] N. Cao, S. Chen, and Z. S. She, Phys. Rev. Lett. **76**, 3711 (1996).
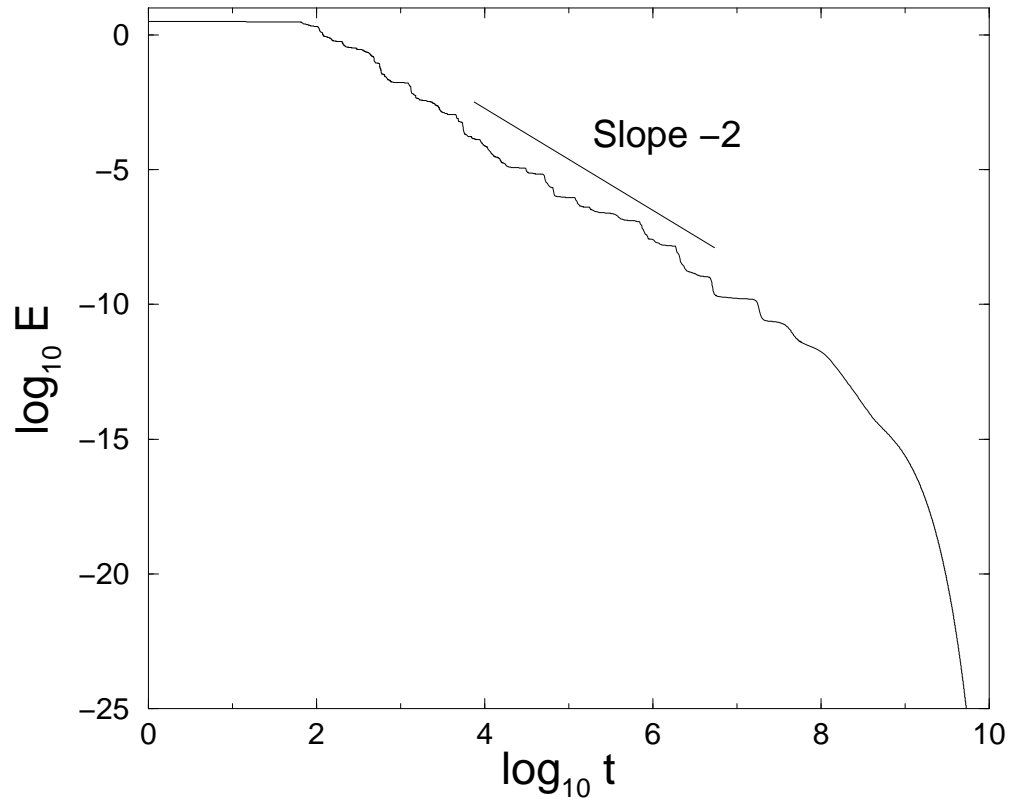[19] N. Schörghofer, L. Kadanoff, and D. Lohse, Physica D **88**, 40 (1995).

FIG. 1. Time decay of the total energy $E(t)$ as a function of time t for one particular realization. Note the step-wise, self-similar behavior. The average slope -2 is also shown.
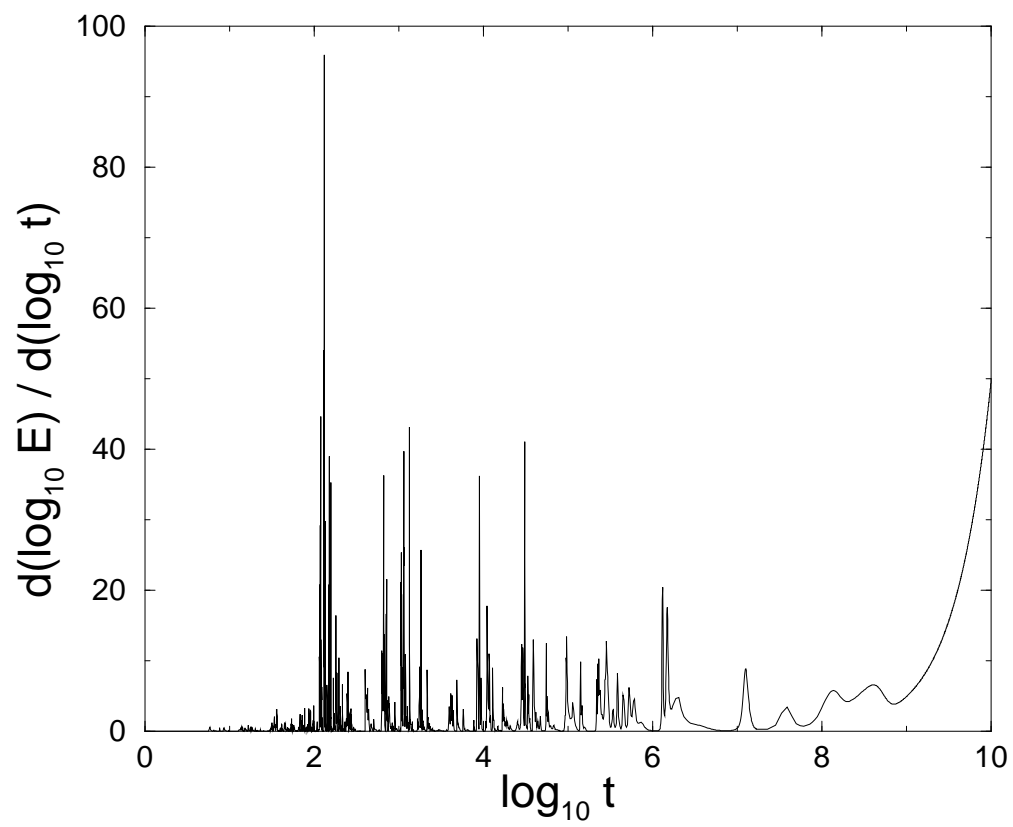
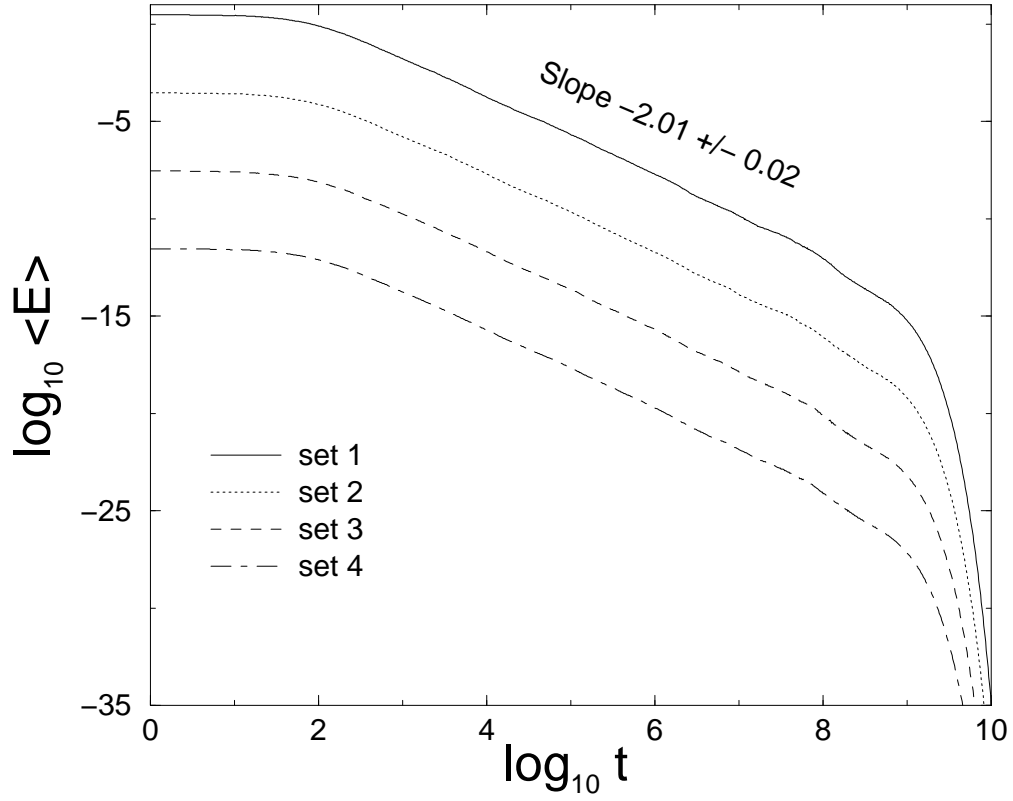FIG. 2. Time derivative of the energy in figure 1.

FIG. 3. Ensemble averaged energy as a function of decay time. In order to give an idea about the statistical error, four sets are shown (shifted in y-direction). Each one is obtained by averaging 500 uncorrelated decay processes.
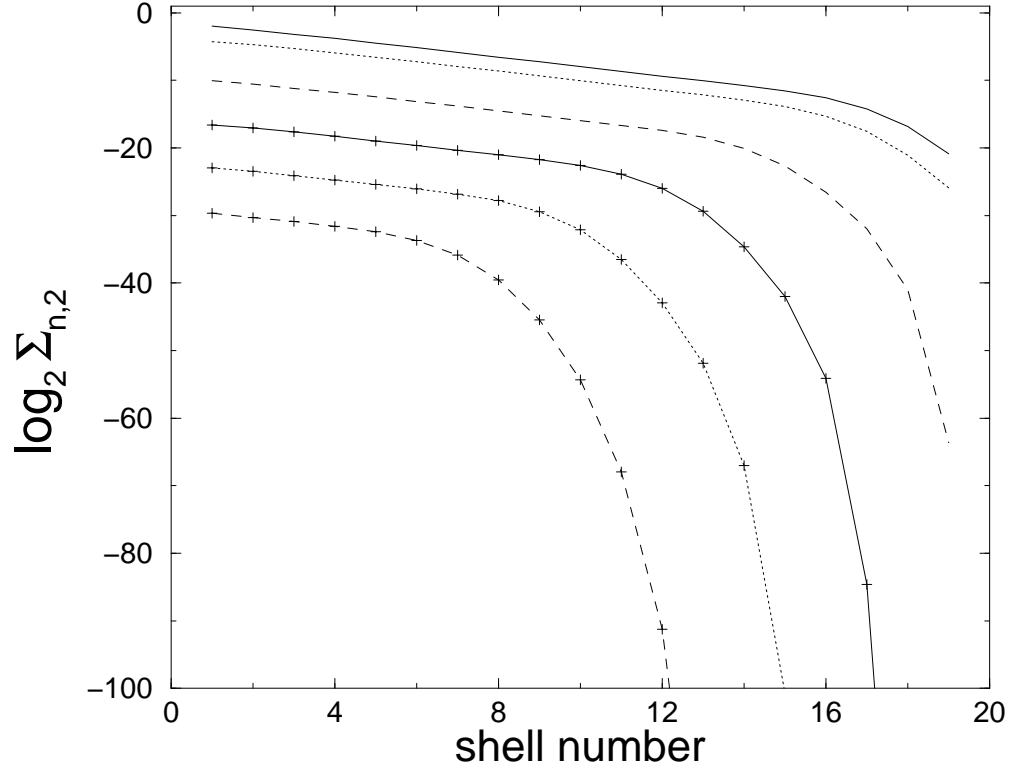
FIG. 4. Second order flux moment $\Sigma_{n,2}$ at six different decay times. The upper curve is the original situation, the following curves reflect the situation one, two, three, four, and five decades in time later. Besides ensemble averaging over 500 ensembles, the respective data are also averaged over one tenth of a decade in time.
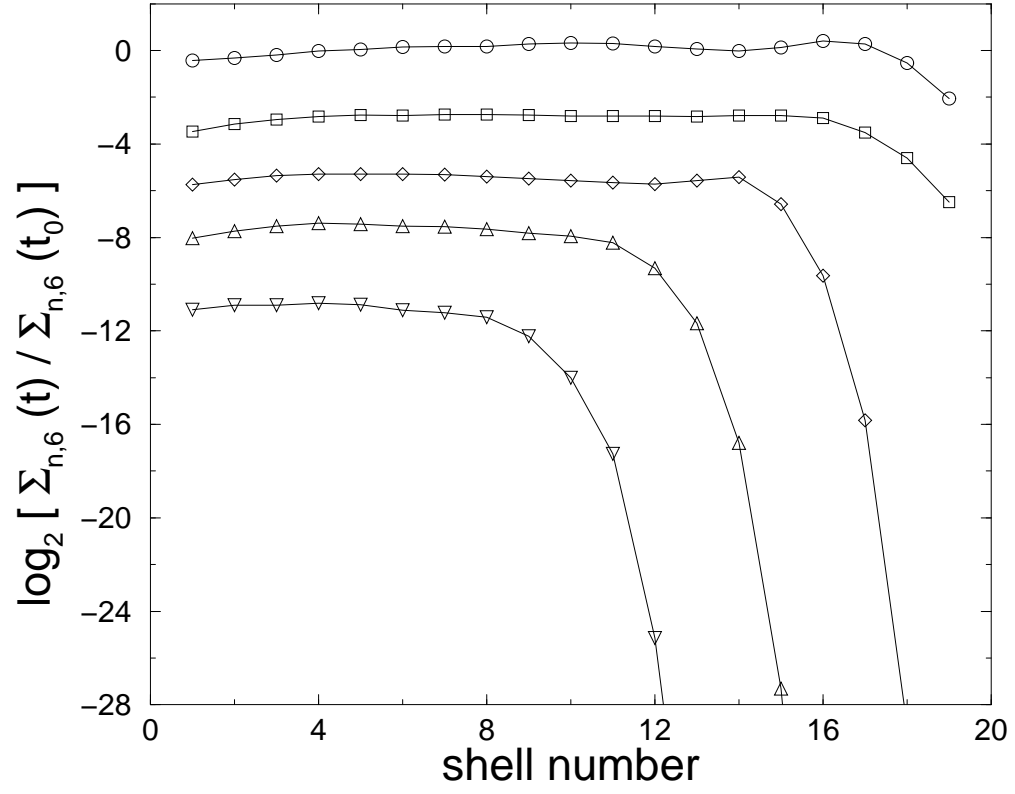
FIG. 5. Ratio of $\Sigma_{n,6}(t)$ to $\Sigma_{n,6}(t_0)$ one, two, three, four, and five decades after t_0 when the decay started. For clarity the curves are again shifted in y-direction.
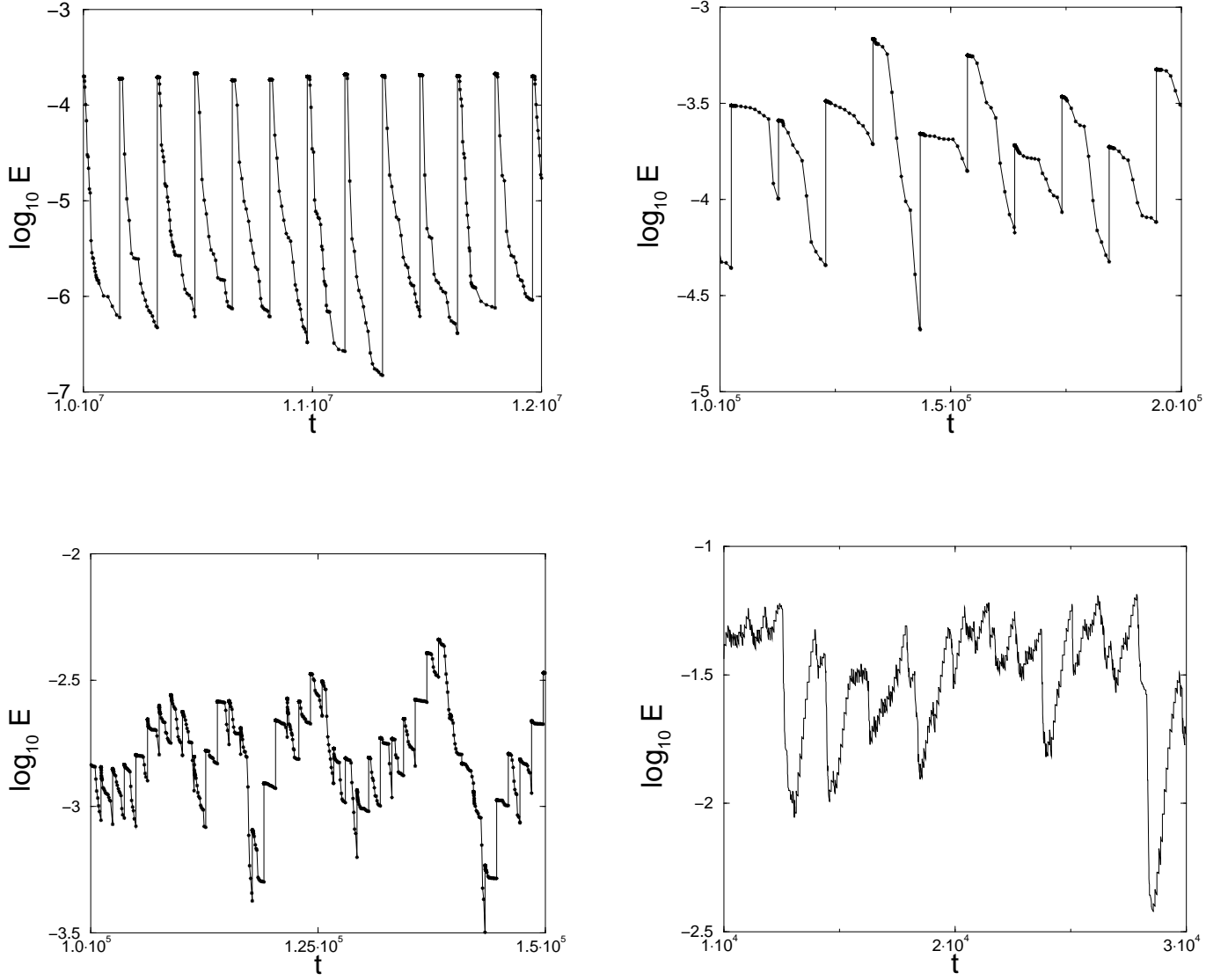
FIG. 6. (Top-Left): Total energy in the GOY as a function of time, in the laminar regime ($f = 6 \cdot 10^{-6}$, $A = 0.01$). (Top-Right): Closely after the laminar regime ($f = 1 \cdot 10^{-4}$, $A = 0.01$). (Bottom-Left): Close to the turbulent regime. ($f = 1 \cdot 10^{-3}$, $A = 0.01$). (Bottom-Right): In the turbulent regime. ($f = 1.5 \cdot 10^{-1}$, $A = 0.01$).
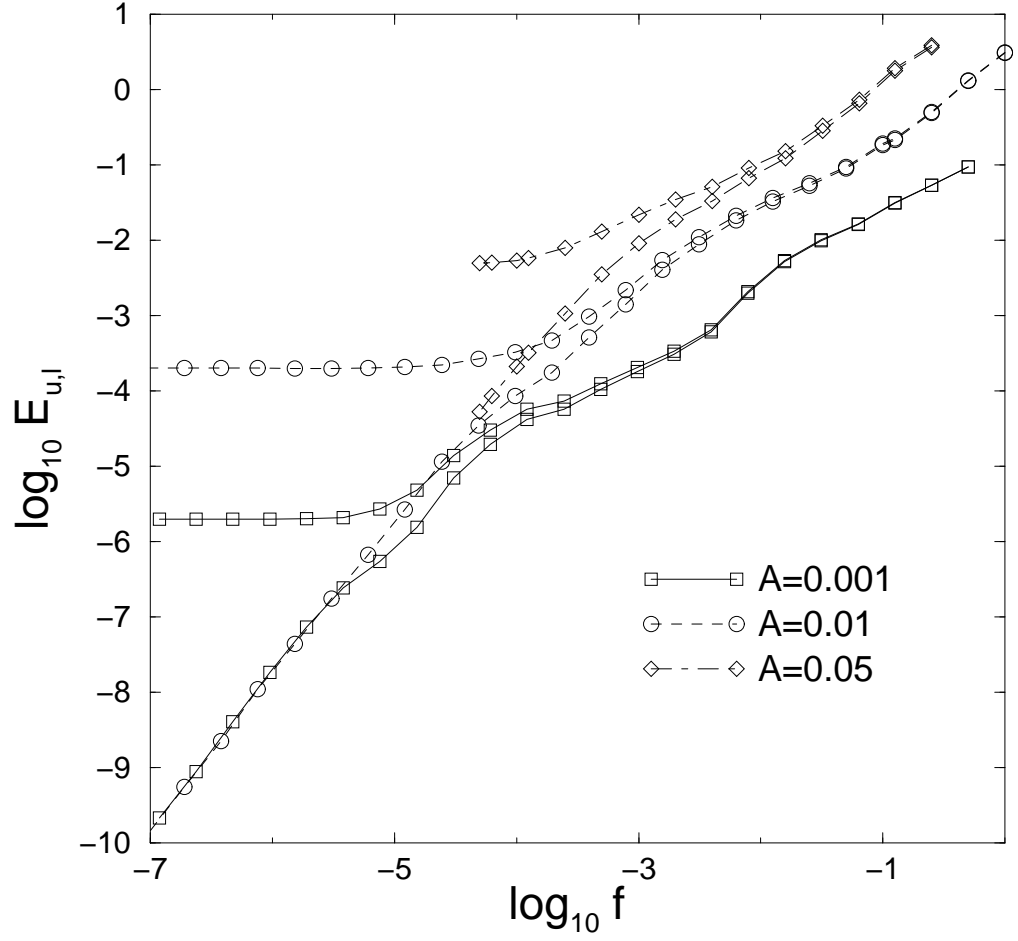
FIG. 7. Numerical computation of the energy levels. E_l (lower curves) and E_u (upper curves) as a function of the frequency f for three different kicking strengths A. For large f the slope is roughly $E_u \sim E_l \sim f$.
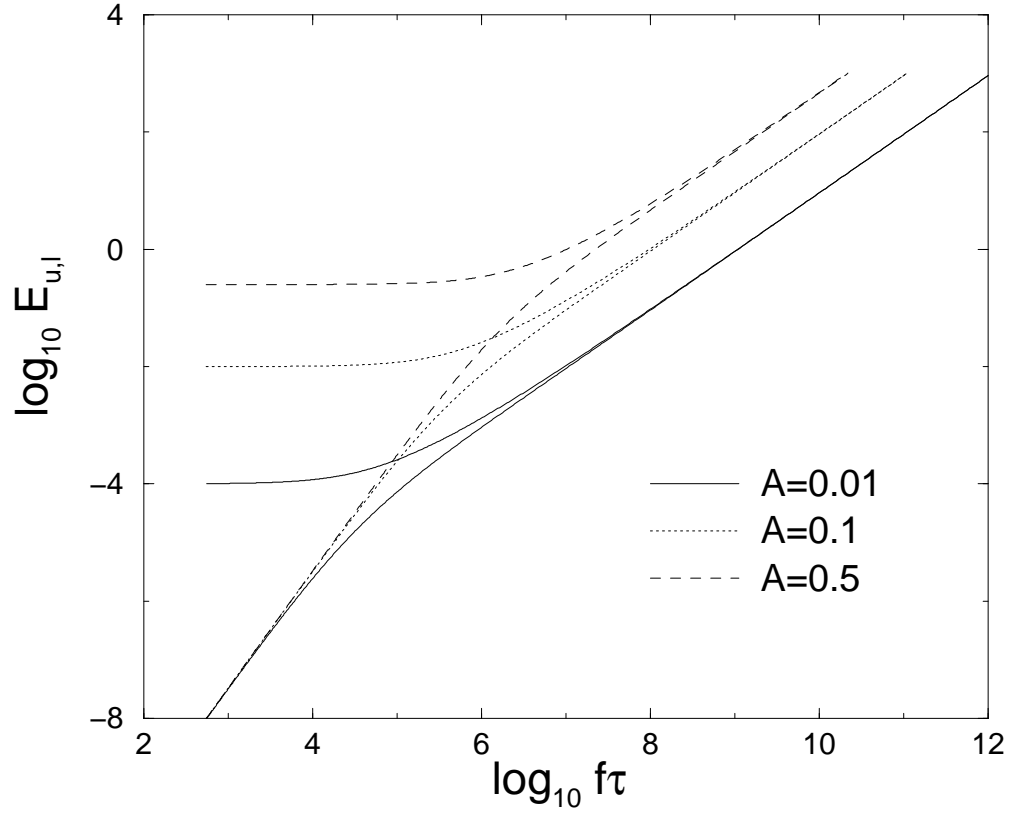
FIG. 8. Energy levels E_u (upper curves) and E_l (lower curves) as a function of the frequency for three different kicking strength, as they follow from the dimensional argument given in the text.